INFECTION AND IMMUNITY, Jan. 2011, p. 75–87 Vol. 79, No. 1
0019-9567/11/$12.00 doi:10.1128/IAI.00815-10

Host DNA Repair Proteins in Response to *Pseudomonas aeruginosa* in Lung Epithelial Cells and in Mice▽

Min Wu,[1]†* Huang Huang,[1]† Weidong Zhang,[1] Shibichakravarthy Kannan,[1] Andrew Weaver,[1] Molynda Mckibben,[1] Danielle Herington,[1] Huawei Zeng,[2] and Hongwei Gao[3]

Department of Biochemistry and Molecular Biology, University of North Dakota School of Medicine and Health Sciences, Grand Forks, North Dakota 58203[1]; USDA, ARS, Grand Forks Human Nutrition Research Center, Grand Forks, North Dakota[2]; and Center for Experimental Therapeutics and Reperfusion Injury, Department of Anesthesiology, Perioperative and Pain Medicine, Brigham and Women's Hospital, Harvard Medical School, Boston, Massachusetts[3]

Received 27 July 2010/Returned for modification 20 August 2010/Accepted 5 October 2010

Although DNA repair proteins in bacteria are critical for pathogens' genome stability and for subverting the host defense, the role of host DNA repair proteins in response to bacterial infection is poorly defined. Here, we demonstrate, for the first time, that infection with the Gram-negative bacterium *Pseudomonas aeruginosa* significantly altered the expression and enzymatic activity of 8-oxoguanine DNA glycosylase (OGG1) in lung epithelial cells. Downregulation of OGG1 by a small interfering RNA strategy resulted in severe DNA damage and cell death. In addition, acetylation of OGG1 is required for host responses to bacterial genotoxicity, as mutations of OGG1 acetylation sites increased Cockayne syndrome group B (CSB) protein expression. These results also indicate that CSB may be involved in DNA repair activity during infection. Furthermore, OGG1 knockout mice exhibited increased lung injury after infection with *P. aeruginosa*, as demonstrated by higher myeloperoxidase activity and lipid peroxidation. Together, our studies indicate that *P. aeruginosa* infection induces significant DNA damage in host cells and that DNA repair proteins play a critical role in the host response to *P. aeruginosa* infection, serving as promising targets for the treatment of this condition and perhaps more broadly Gram-negative bacterial infections.

The DNA repair system of bacteria is important for maintaining the genostability of pathogens (46) and for subverting the host defense (59), but the host's DNA repair response to bacterial invasion is poorly understood. A rough picture has recently emerged from studies of *Helicobacter pylori* infection, in which an accumulation of reactive oxygen species (ROS) in gastric mucosa (11) induces oxidative DNA damage and subsequent DNA repair responses (11, 13, 34). However, little is known about the responses to bacterial infection in the respiratory tract. *Pseudomonas aeruginosa*, a Gram-negative bacterium, is a typical opportunistic human pathogen that can infect almost any tissue and is especially damaging to the respiratory system. *P. aeruginosa* accounts for 10.1% of all hospital-acquired infections, frequently occurring in immunoimpaired conditions, such as ventilator-associated infection, burns, and cancer, as well as in almost all cystic fibrosis patients (6, 22, 85). In patients with impaired immune functions, *P. aeruginosa* breaks respiratory boundaries causes in persistent or severe infections. Although DNA repair proteins such as X-ray repair cross-complementing 1 (XRCC1) may participate in immunity in myeloma (17), the role of DNA repair proteins in the immune system response to respiratory infection remains unresolved.

The primary outcome of *P. aeruginosa*-induced toxicity in host cells was thought to be apoptosis (57). Respiratory apoptosis may occur through caspase 8 (1) and the CD95 death receptor (15). However, this bacterium-induced apoptosis is a subject of controversy because an early report of bacterial apoptosis in mouse lungs could not be reproduced by other groups (23, 54). Thus, the ultimate outcome of *P. aeruginosa* infection remains to be defined. *P. aeruginosa* employs various virulence factors, such as exotoxin A, pyocyanin, and lipopolysaccharides (LPS), to induce host cell apoptosis (1, 28), resulting in tissue injury. For example, exoenzymes such as ExoS and ExoT target host cytoskeleton proteins and disrupt respiratory barriers (65), whereas ExoU and exotoxin A may induce oxidation or stimulate host cells to release ROS (54, 61). To make the matter worse, excessive host-secreted inflammatory cytokines (tumor necrosis factor alpha [TNF-α]) may also induce genotoxicity (62). Of these, 7,8-dihydro-8-oxoguanine (oxoG) is the most common form of oxidative DNA adduct (10) and tends to mispair with the base A (adenine), leading to a mutagenic transversion of GC to TA (8, 16, 63).

One essential repair pathway capable of removing oxidized nucleotide precursors like oxoG, and therefore potentially involved in the host response to *P. aeruginosa*, is base excision DNA repair (BER). The BER pathway begins with a glycosylase action by 8-oxoguanine DNA glycosylase (OGG1) to cleave oxoG. The orthologs for OGG1 in *Escherichia coli* are formamidopyrimidine DNA glycosylase (Fpg) and endonuclease VIII (Nei), which have similar three-dimensional structures, as well as homology in conserved structural motifs (40). However, Fpg and Nei show different substrate specificities: Fpg proteins recognize formamidopyrimidines, oxoG, and its oxidation products guanidinohydantoin and spiroiminodihydantoin, while bacterial Nei proteins recognize primarily dam-

* Corresponding author. Mailing address: Department of Biochemistry and Molecular Biology, University of North Dakota School of Medicine and Health Sciences, Grand Forks, ND 58203. Phone: (701) 777-4875. Fax: (701) 777-2382. E-mail: min.wu@med.und.edu.
† Co-first authors.
▽ Published ahead of print on 18 October 2010.

aged pyrimidines (25). Nei-like 1 (NEIL1) in mammals may serve as a backup for OGG1 (40). OGG1 attacks the N-glycosidic bond using the active-site Lys249 nucleophile to form a transient Schiff base. After the base lesion is removed, the bound enzyme exerts the lyase function via β elimination to cleave the DNA strand at the damage site and produces 3′-phospho-α-β-unsaturated aldehyde and 5′ phosphate termini, forming an apurinic/apyrimidinic (AP) site (21, 45). This AP site is then nicked by AP endonuclease 1 (APE1, APN1 is a homolog in yeast), and DNA strand extension is accomplished by polymerase β and ligated by ligase I (18, 19, 75). APE1 can activate OGG1 activity without physical interaction. Since APE1 is also a typical redox protein and is involved in various cellular oxidation processes (21), it may be activated by proinflammatory cytokines during infection. OGG1a, the main functional isoform, is localized in nuclei, while other isoforms (OGG1b and -c and OGG2) are found in mitochondria (49). Phosphorylation of OGG1 regulates its glycosylase activity (24), whereas acetylation of OGG1 may enhance its efficiency in repairing oxoG (5). To effectively repair damaged DNA, the BER pathway also interacts with various DNA repair proteins or cell signaling proteins, such as poly(ADP-ribose) polymerase 1 (PARP1) and XRCC1 (25, 37). PARP1, in particular, has been reported to regulate inflammatory responses in OGG1-deficient mice (39). Although BER proteins are the recognized enzymes for repairing oxidative DNA damage, nuclear excision repair (NER) proteins such as Cockayne syndrome group B (CSB) may also interact with PARP1 (69) or OGG1 to carry out oxidative DNA repair (68, 71). Xeroderma pigmentosum B (XPB) also contributes to DNA repair upon oxidative stress (58). Using a neurodegenerative rabbit model with a cholesterol-rich diet, we have demonstrated that OGG1 interacts with XPB in the brain (76).

We hypothesized that infection with *P. aeruginosa* induces DNA damage, which in turn initiates DNA repair responses to reverse this damage. To test this hypothesis, we investigated the DNA repair response following *P. aeruginosa* infection in alveolar epithelial cells and in OGG1 knockout (KO) mice. We demonstrated that oxidative stress induced by multiple bacterial components could contribute to DNA damage and initiate a broad range of DNA repair responses in the host, particularly the BER pathway response. Our data indicate that by interacting with other host defense mechanisms, OGG1 helps reduce pathogen-induced DNA damage and subsequent cell death. In addition, we determined the role of NER proteins (XPB and CSB) during infection, and our data suggest that these NER proteins may also participate in the host response through interaction with OGG1.

MATERIALS AND METHODS

Cells. Human epithelial A549 and mouse epithelial MLE-12 cells, considered to be of alveolar epithelial cell type II (AECII), were purchased from the American Type Culture Collection, Manassas, VA. A549 cells were maintained in Dulbecco's modified Eagle's medium (Cellgro Mediatech Inc., Herndon, VA) containing 10% newborn bovine serum (NBS; Highclone, Logan, UT). Mouse AECII cells were isolated from female C57BL/6 mice (Harlan, Indianapolis, IN) as previously described (32, 33).

Bacterial strains. Wild-type (WT) *P. aeruginosa* strain PAO1 was obtained from Stephen Lory (Harvard Medical School, Boston, MA). Green fluorescein protein (GFP)-expressing PAO1 and PAK were kindly provided by Gerald Pier (Harvard Medical School) (55). The type three toxin PAO1 mutants ΔExoS and ΔExoT used in this study were graciously provided by J. Barbieri (Medical College of Wisconsin, Milwaukee) (84). The bacteria were grown overnight in LB broth at 37°C while shaken at 220 rpm until the mid-logarithmic phase of growth (30, 31). Mammalian cells were infected with a multiplicity of infection (MOI) of 10:1 in most cases for 1 h or for different time periods. The bacteria were then removed by washing with phosphate-buffered saline (PBS), and fresh medium containing conventional (penicillin-streptomycin, 100 U/ml and 100 μg/ml, respectively) and additional antibiotics (polymyxin B, 200 μg/ml) was added for another 1 h of incubation before further analysis. No adverse effects were observed in the cells after infection. Blockade of DNA damage was performed with the lipid raft inhibitor methyl-β-cyclodextrin (mβCD, 10 mM), Lyn kinase (PP2, 5 μg/ml), MEK-ERK1/2 (U0126, 2.5 μg/ml; Calbiochem), and vehicle (dimethyl sulfoxide [DMSO; used as a reagent diluent]) 30 min before infection with PAO1.

RNA extraction and analysis. RNA was extracted from cells using RNA easy kits (Qiagen, Valencia, CA). Reverse transcription (RT)-PCR was performed using the Titan one-step RT-PCR kit (Roche Molecular Biochemicals, Indianapolis, IN), and samples of 0.2 μg of total RNA were used as templates (52, 78).

Transfection and transduction. The pcDNA-OGG1 construct was cloned by the insertion of full-length OGG1 cDNA into the pcDNA3.1 vector (79). An internal ribosome entry site (IRES) that contains a GFP vector (pIRES-GFP) expressing OGG1 was created by inserting OGG1 into the pIRES vector (Clontech Laboratories, Mountain View, CA) (79, 81). A549 cells were infected with our pSF91 retroviral vector expressing OGG1 and screened to obtain stable single colonies expressing high levels of OGG1 as described previously (79). OGG1-FLAG, OGG1-His, and OGG1 acetylation site mutant (K338R/K341R) constructs were kindly provided by T. Hazra (University of Texas Medical Branch at Galveston) as described previously (5). For small interfering RNA (siRNA) transfection, a pool of four specific siRNAs against OGG1 or sense controls were purchased from Dharmacon, West Lafayette, CO (catalog no. M-003153-0005 and D-001206-1305), and transfected in accordance with the manufacturer's instructions.

Comet assay. The comet assay was conducted using a CometAssay kit (Trevigen, Gaithersburg, MD) as previously described (29, 33). The cells were infected with *P. aeruginosa* or medium controls as indicated above and were washed with Ca^{2+}- and Mg^{2+}-free PBS. The cells were gently dissociated from the plate at a concentration of 3×10^5/ml. A small aliquot of this mixture (cells and liquefied agarose at a 1:10 [vol/vol] ratio) was immediately transferred onto slides. After lysis of the cells at 4°C, the slides were exposed to alkali solution (0.3 M NaOH, 1 mM EDTA) for 30 min to unwind the double-stranded DNA and electrophoresed at 1 V/cm for 20 to 30 min to obtain a desired result. Following SYBR staining, the samples were photographed using a Zeiss LSM510 fluorescence microscope. The lengths of comet tails are proportional to the abundance of damaged DNA fragments and are determined as the distance between the leading edge of the nucleus and the ending edge of the cell (under fluorescence staining). About 100 cells were counted for each sample using the CometScore software (Trevigen).

DNA repair activity assay. The activity of DNA repair proteins in cleaving specific target nucleotides was assessed using radiolabeled oligonucleotide substrates as described previously (79). The OGG1 activity of transduced cells was quantified by detecting the cleavage of the following 23-bp oligonucleotide substrate containing a single 8-oxoguanine lesion (in bold): 5′-GAA-CTA-GTG**O**ATC-CCC-CGG-GCT-GC-3′ (Trevigen). Lysates from control cells and cells transduced with OGG1 (10-μg protein samples) were reacted separately with 0.1 pmol of the [γ-^{32}P]dATP-end-labeled 23-bp substrate at 37°C for 1 h in analysis buffer. The reaction was terminated by addition of 90% formamide loading buffer, and the samples were separated by denaturing sodium dodecyl sulfate (SDS)-polyacrylamide gel (20%) electrophoresis. After X-ray film images had been acquired, data were determined by densitometric analysis using the Adobe Photoshop software (79).

Immunochemical analysis. Epithelial cells were grown on plain or collagen (human type IV; Sigma-Aldrich)-coated coverslips (Nalge Nunc International, Rochester, NY). After infection, cells were fixed in 3.5% paraformaldehyde, permeabilized with 0.1% NP-40 (Sigma-Aldrich) in PBS, and blocked with blocking buffer (PBS containing 1% NBS and 0.1% NP-40) for 30 min (31). Cells were incubated with primary antibodies at a 1:500 dilution in blocking buffer for 1 h and washed three times. After incubation with appropriate fluorophore-conjugated secondary antibodies, images were captured with an LSM 510 Meta confocal microscope (Carl Zeiss MicroImaging, Inc., Thornwood, NY). Differential interference contrast pictures were taken simultaneously with fluorescence images (31).

Quantification of imaging data. The intensity and average sizes of fluorescent staining samples were quantified using the "analyze particle" plug-in function of

the ImageJ software (NIH) (31). Briefly, the images were converted into 8-bit format and then a threshold intensity of 50% was applied to the green channel. This threshold helped to remove any unwanted background. The regions being assayed were highlighted by selecting with region-of-interest tools.

Nuclear extraction. Cells were lysed with 400 μl of lysis buffer (10 mM HEPES [pH 7.5], 10 mM KCl, 2 mM $MgCl_2$, 1 mM EGTA, 1 mM EDTA, 1 mM dithiothreitol [DTT], 10 mM NaF, 0.1 mM Na_3VO_4, protease inhibitor cocktail). The cells were incubated for 15 min on ice with gentle shaking, 25 μl of 10% NP-40 was added, and the mixture was mixed carefully and incubated on ice for 5 min. The lysates were centrifuged for 30 s at 13,000 rpm to pellet the nuclei. The supernatant (cytosol) was transferred to a new tube. Fifty microliters of nuclear extraction buffer (25 mM HEPES [pH 7.5], 5 mM $MgCl_2$, 500 mM NaCl, 1 mM DTT, 10 mM NaF, 0.2% NP-40, 10% glycerol) was added to the pellet, and the sample was briefly sonicated twice and centrifuged for 5 min at 13,000 rpm to obtain nuclear extracts (supernatant). The histone 1 protein was probed as a marker for nuclear proteins, and tubulin was used as a marker for cytosol or whole lysate.

Western blotting and coimmunoprecipitation. The samples of cells and lung homogenates were lysed and quantified. The lysates were boiled for 5 min after protease inhibitors had been added. The supernatants (30 μg of each sample) were loaded onto 10% SDS-polyacrylamide minigels and electrophoresed to resolved proteins. For the detection of pro-SP-C (antibodies from J. A. Whitsett, Cincinnati, OH) and PARP1 (obtained from Neomarkers, Fremont, CA), a nonreducing condition was used. Proteins were then transferred from gels to polyvinylidene difluoride membranes (Pierce Biotechnology, Rockford, IL) and blocked overnight at 4°C with 5% nonfat milk blocking buffer (32). Membranes were incubated overnight at 4°C with the appropriate primary antibodies. The primary antibodies (to OGG1, APE1, CSB, XPB, and glyceraldehyde 3-phosphate dehydrogenase [GAPDH]) were obtained from Santa Cruz and diluted 1:1,000. XRCC1 was purchased from Neomarkers. After being washed three times with Western washing solution, the membranes were incubated for 2 h at room temperature with horseradish peroxidase-conjugated secondary antibody (Amersham, St. Louis, MO, or Santa Cruz Biotechnology) diluted 1:2,000 (83). Signals were visualized using an enhanced chemiluminescence detection kit (SuperSignal West Pico; Pierce).

For coimmunoprecipitation, the supernatants were precleared with bare protein A/G-Sepharose beads (Santa Cruz Biotechnology) for 1 h at 4°C and then incubated with anti-OGG1 antibodies (Santa Cruz Biotechnology or Novus) bound to protein A/G-Sepharose beads overnight at 4°C (31, 33). The beads were then washed three times in lysis buffer and boiled after SDS sample loading buffer had been added. The proteins were then separated and analyzed by Western blotting.

Lung sections. C57BL/6 mice (Jackson Laboratories, Bar Harbor, ME) were used to study bacterium-induced oxidation in animals (80, 82). Infection was performed intranasally, and the free bacteria were washed off with saline. The lungs were then perfused and inflated with optimum compound temperature (OCT). Cryosections were made using cryostat (Tissue-Tek, Elkhart, IN). Tissue sections were fixed with ice-cold acetone for 10 min. Immunofluorescence staining was performed as described above. Groups of five mice each were used. Hematoxylin-and-eosin (H&E) staining was performed using a standard procedure.

Cell proliferation [3-(4,5-dimethylthiazol-2-yl)-2,5-diphenyltetrazolium bromide (MTT)] assay. Cell Titer 96 Non-Radioactive Cell Proliferation Assay kits (Promega, Madison, WI) were utilized to evaluate cell survival following infections (77). Equal numbers of cells (5,000/well) were loaded into all wells for infection or other treatments and assayed according to the manufacturer's instructions.

Apoptosis assays. Apoptosis of cultured cells was determined 2 h after infection by using the Vybrant assay (Molecular Probes, Carlsbad, CA) according to the manufacturer's protocol (32). Apoptotic cells were stained with the green dye YO-PRO1, while necrotic cells were stained with the red dye propidium iodide. The results could then be determined with either fluorescence microscopy or a fluorescence plate reader, which can differentiate the death patterns. Hydrogen peroxide (100 μM), which is known to cause DNA damage, was used as a positive control to induce necrosis and apoptosis as described previously (29).

Lipid peroxidation assay. Homogenized lung tissues were dissolved in 62.5 mM Tris-HCl (pH 6.8) supplemented with Complete-Mini Protease Inhibitor (Roche Diagnostics) or in PBS in equal protein amounts. Lipid peroxidation was measured by thiobarbituric acid-reactive substance colorimetric assay as described previously (51). Tetramethoxypropane was used as a standard of quantification, and data were expressed as micromolar per gram of protein.

Lung myeloperoxidase (MPO) assay. The MPO assay was performed as previously described (44). Lung tissue samples were homogenized in 50 mM hexadecyltrimethylammonium bromide–50 mM KH_2PO_4 (pH 6.0)–0.5 mM EDTA–1 ml/100 mg tissue and centrifuged for 15 min at 12,000 rpm at 4°C. Supernatants were decanted, and 100 μl of reaction buffer (0.167 mg/ml *O*-dianisidine, 50 mM KH_2PO_4 [pH 6.0], 0.0005% mM H_2O_2) was added to 100 μl of sample. Absorbances were read at 460 nm at 2-min intervals.

Statistical analysis. Group means were compared by Student's *t* test or one-way analysis of variance (ANOVA), followed by the Turkey's post-hoc analysis, using SigmaStat software, and significant difference was accepted at $P < 0.05$.

RESULTS

DNA damage responses in respiratory cells to *P. aeruginosa*. Since A549 cells possess the characteristics of AECII and are widely used as a model system (33, 48, 66, 74, 81), we chose the cell line as the host cells to examine bacterium-induced DNA damage by PAO1, a laboratory strain. The DNA damage was quantified by comet assay, which can detect DNA single-strand breaks as part of the general migration of nuclear components during the electrophoresis of a lysed eukaryotic cell (70). The lengths of comet tails in this assay are proportional to the abundance of damaged DNA fragments, thus indicating the extent of DNA damage. We show that PAO1 infection markedly increased DNA strand breaks compared to controls (Fig. 1A). After exposure to PAO1 for 1 h, the average tail length was 14.8 ± 1.7 μm (arbitrary units) in infected cells but only 1.2 ± 0.21 μm in control cells ($P < 0.01$). To examine whether *P. aeruginosa* infection is a general inducer of genotoxicity, we also tested DNA damage induced by an alternative strain, PAK, and found that significant DNA damage was also induced (data not shown). To account for species factors, we examined DNA damage in the murine epithelial cell line MLE-12 and found that PAO1 induced similar extents of DNA damage in these cells (data not shown). It should be noted that a comet assay may enumerate DNA damage derived from both the host and the pathogen. Although a comet assay cannot discriminate the DNA types of different species, the bacterium's genome is a fraction of the size of the host's, and therefore the comet assay would not be sensitive enough to detect damaged prokaryotic DNA. Also, the number of internalized bacteria is relatively small and adherent bacteria may also be insignificant after high-dose antibiotic treatment and extensive washing.

While the classical comet assay may only detect DNA strand breaks, preincubation with a glycosylase (purified His-OGG1) can convert DNA base damage into open ends within DNA strands, allowing the formation of fully broken strands during an unwinding process. We used this method to detect DNA base damage rather than strand breaks, and we found that these preincubated samples showed an approximately 2-fold increase in base DNA damage (e.g., oxoG) after PAO1 infection for 1 h compared to medium-only controls (data not shown). Interestingly, levels of DNA damage correlated with the amount of bacteria (Fig. 1B); i.e., increasing bacterial loads induced longer comet tails. We also found that infection did not cause apparent strand breaks at earlier times (up to 5 min) but induced apparent strand breaks at later times (data not shown). Thus, the bacterium-induced DNA damage is dose and time dependent. These damage patterns are similar to those reported for gastroenterological epithelial cells under *H. pylori* infection (11), as well as for lung cells exposed to hyperoxia (2).

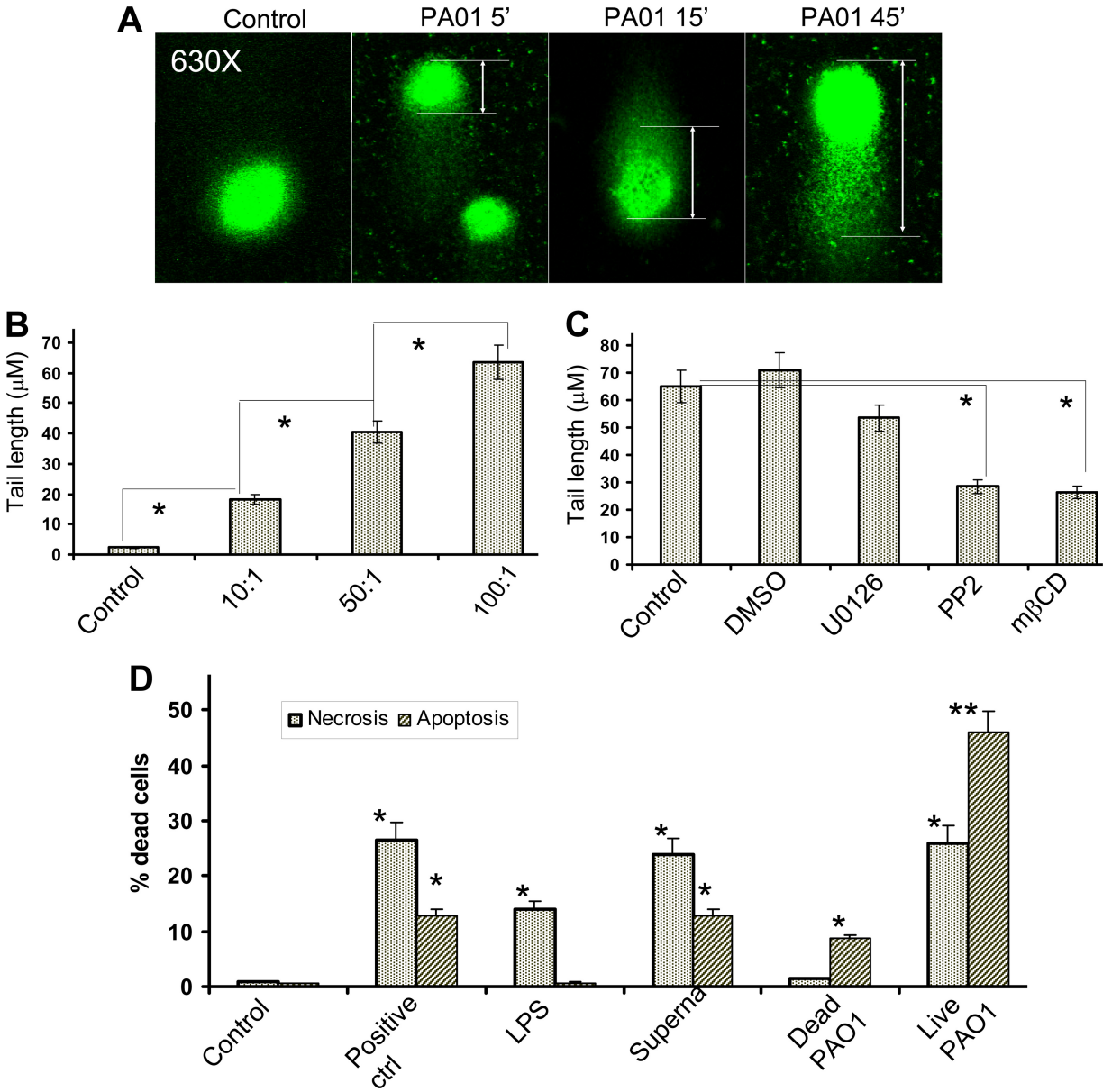

FIG. 1. Induction of DNA damage and cell death by PAO1. (A) Time-dependent DNA damage. A549 cells were infected with PAO1 (MOI, 10:1) for various durations, and DNA damage was determined by comet assay after rewinding the DNA with alkaline buffer. Slides were stained with SYBR and viewed using fluorescence microscopy (see Materials and Methods). The control contained no bacteria. (B) Bacterial load-dependent DNA damage. A549 cells were infected with various amount of PAO1 for 1 h, and tail lengths (indicated by rulers) were measured by CometScore software (100 cells counted/sample) (*, $P < 0.05$, confidence interval [CI] 95%). The *x* axis shows various MOIs. (C) Reduction of DNA damage by blocking Lyn kinase (PP2, 5 nM) and lipid rafts (mβCD, 10 mM) as determined by comet assay. However, the vehicle (DMSO at 5 nM as a dilution reagent) and MEK-ERK1/2 inhibitor (U0126, 2.5 μM) had no effects on PAO1-induced DNA damage. In addition, PP2 and mβCD alone had no effects on tail lengths compared to the control (not shown). (D) Quantitative assays of apoptosis and necrosis. LPS (serotype 10, 200 ng/ml), supernatant of PAO1, and live PAO1 were incubated with AECII cells for 1 h, and the bacteria and reagents were replaced with fresh medium containing antibiotics. Hydrogen peroxide (100 μM) served as the positive control (ctrl) for necrosis and apoptosis. The cells were further incubated for 18 h and assessed by Vybrant assay (one-way ANOVA; *, $P < 0.05$, CI 95%; **, $P < 0.01$, CI 99% [all compared to the control]). The data shown are representative of three experiments.

Upon the adhesion or attachment of bacteria to host membranes or absorption of secreted toxic substances, the host cells may undergo rapid membrane reorganization, receptor clustering, and compartmental segregation (64). Membrane compartmental segregation, involved in the aggregation of lipid rafts, transmits cell signals and impacts the outcome of infection. This segregation can either strengthen innate immunity by activating Toll-like receptors or dampen the host response through a raft-hijacking mechanism (41). Increasing evidence indicates that cellular signals serve as an intermediate in linking lipid rafts to DNA repair in response to multiple stresses (38). To elucidate the possible involvement of membrane raft-

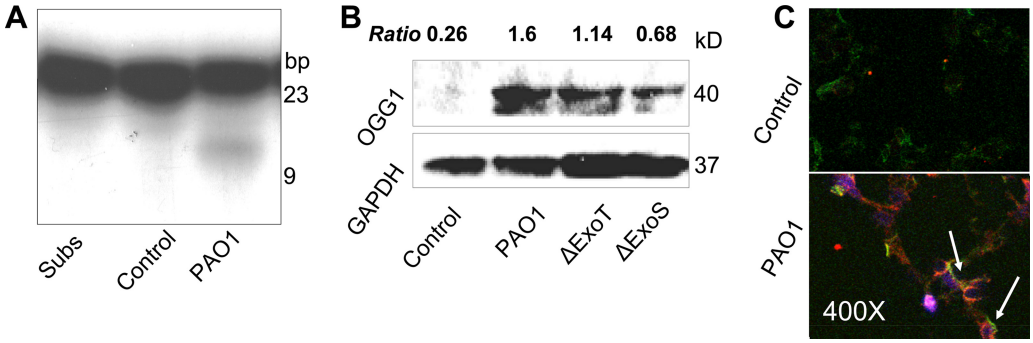

FIG. 2. Responses of DNA repair proteins to PAO1 infection. (A) Increased OGG1 activity as determined by incision enzymatic assay. A549 cells were infected with PAO1 for 1 h and lysed for isolation of nuclear extract. Subs, substrate only; control, untreated cells. Ten micrograms of cell extract was reacted with 2.5 pM [γ-^{32}P]ATP-labeled 8-oxoguanine containing a 23-bp oligonucleotide for 60 min at 37°C, and the reaction solution was resolved by 7 M urea denaturing gel electrophoresis. The cleaved substrate appeared as a 9-bp band. (B) Induction of OGG1 protein expression by PAO1 infection assessed by Western blotting. One hour after infection with PAO1 or a ΔExoT or ΔExoS T3SS secretion mutant, the bacteria were removed and A549 cells were then cultured continually for 18 h before probing with OGG1 antibodies (Santa Cruz). GAPDH was probed for in the same gel to show loading. The OGG1 quantity was determined as a ratio (OGG1 divided by loading) using densitometry (Bio-Rad Quantity One). (C) DNA repair response to 24 h of PAO1 infection in mouse lungs. PAO1 (10^7 CFU) was intranasally instilled into C57BL6 mice, and the lungs were removed after lavage to remove the free bacteria. Cryosections were then stained with antibodies against OGG1 and oxoG. OGG1 stained with TRITC was colocalized with oxoG (FITC) (arrows, colocalization of OGG1 with the DNA adduct oxoG). The data shown are representative of three experiments.

initiated signals in DNA damage, we used a lipid raft blocker (mβCD) and a Lyn kinase (a raft-resident protein) chemical inhibitor (PP2) to disrupt these signals. Our data show that these inhibitors (mβCD and PP2) significantly reduced bacterium-induced DNA damage, whereas a MEK-ERK1/2 inhibitor (U0126) had no apparent effects on PAO1-induced DNA damage (Fig. 1C). In addition, the vehicle control (DMSO), mβCD, and PP2 alone did not inhibit DNA damage (data not shown). This finding indicates that the lipid raft-mediated signals may also be involved in DNA damage induced by virulence factors.

Since severe DNA damage may lead to cell death, we further examined the characteristics of cell death using a Vybrant assay to distinguish between apoptosis and necrosis. LPS (200 ng/ml, serotype 10; Sigma) were used, along with the bacterium, to induce oxidative cytotoxicity. LPS and supernatant of PAO1 induced stronger necrosis (propidium iodide staining) than did dead PAO1 or live PAO1, but the latter caused significant apoptosis (green staining), as determined by Vybrant assay quantified by fluorescence microscopy. Previous reports suggest that LPS induced TNF-α production, an inflammatory response, thereby resulting in necrosis (56), which is consistent with our observation. Dead bacteria may trigger host responses through surface structural components such as pili (9), whereas live bacteria may induce host genotoxicity through a variety of virulence factors, including type III secretion system (T3SS) toxins, surface structures, etc. Live bacteria caused the strongest apoptosis among these agents, suggesting that host-pathogen interaction may also contribute to the cytotoxicity seen (Fig. 1D).

DNA repair response upon *P. aeruginosa* infection. *P. aeruginosa*-induced DNA damage may induce responses by different DNA repair proteins, recruiting them to the damage site to recognize and repair the DNA lesion. As oxidative DNA damage is primarily repaired by the BER pathway, we began to dissect the involvement of OGG1, the initiator of this pathway. We looked for increases in OGG1 enzymatic activity using a radiolabeled oligonucleotide(s) containing an oxo lesion in guanine (79). We found that OGG1 activity upon *P. aeruginosa* infection was significantly greater, 5-fold (5.41 ± 0.05), than that in the controls (Fig. 2A), as determined by densitometry (Bio-Rad Quantity One). Western blotting also showed that the expression of OGG1 was increased by more than 6-fold (6.15 ± 0.13) over the control as measured 1 h after *P. aeruginosa* infection (Fig. 2B). *P. aeruginosa* utilizes multiple virulence factors in invasion to cause tissue damage or induce a severe inflammatory response. For example, bifunctional cytotoxic exoenzymes (ExoS and ExoT) may help the bacterium subvert the host's immunity through N-terminal GTPase-activating protein and C-terminal ADP-ribosyltransferase activities. To probe the role of exoenzymes in genotoxicity, we infected cells with exoenzyme-deficient strains (PAO1 ΔExoS and ΔExoT, the strains described in Materials and Methods) (67). Both the ΔExoS and ΔExoT mutants showed less induction of OGG1 expression, with the reduction being much more pronounced in the ΔExoS strain (6.5-fold versus 2.6-fold by WT PAO1 [$P < 0.01$, one-way ANOVA]). To define the physiological relevance of OGG1-mediated DNA repair, we infected C57BL6 mice and found that a DNA repair response was also induced by PAO1 infection in mouse lungs compared to saline controls (Fig. 2C). Further, OGG1 (tetramethyl rhodamine isothiocyanate [TRITC]) was colocalized with the DNA adduct oxoG (fluorescein isothiocyanate [FITC]) in infected lungs of C57BL/6 mice. Analysis of this colocalization showed that the average intensity (of fluorescence) is 5.5-fold greater than in controls, as analyzed using ImageJ software. Furthermore, the number of colocalized regions is markedly increased (40.4 to 1) by PAO1 infection versus the saline control. This novel discovery demonstrated that OGG1 is increased following bacterial infection. Thus, our observations indicate that oxoG may be involved in lung injury and that OGG1 may have a role in mitigating this injury.

AECII as a major responder to *P. aeruginosa* infection. Since AECII plays a key role in protecting the lungs from constant

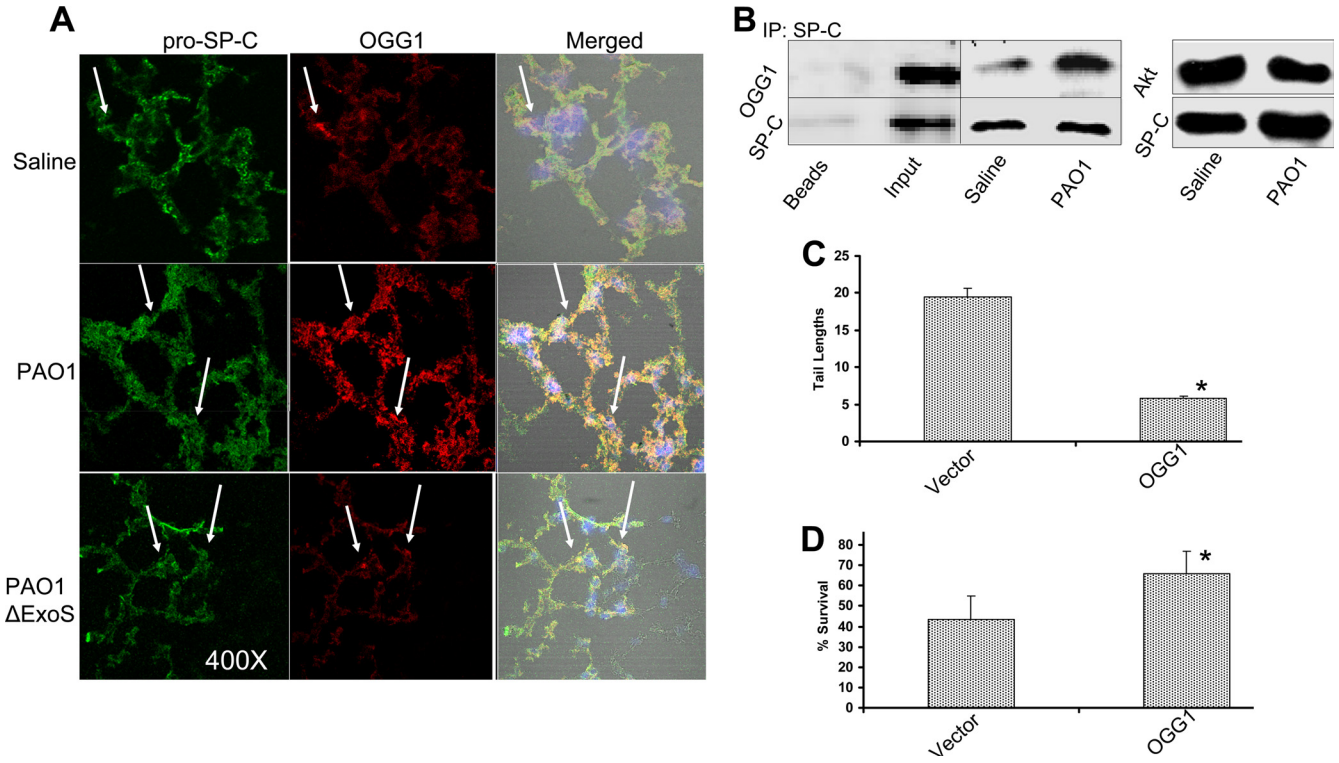

FIG. 3. PAO1-induced OGG1 expression in AECII cells. (A) OGG1 expression in lung AECII cells as identified by indirect immunofluorescence. Cryosections of mouse lungs infected with PAO1 for 18 h were stained with antibodies against OGG1 (red) or pro-SP-C (green) (each staining and colocalization indicated with arrows). (B) Identification of specific OGG1 expression in AECII cells by coimmunoprecipitation (IP). Isolated AECII cells from female C57BL/6 mice were infected with PAO1, and cell lysates were pulled down with pro-SP-C antibodies and probed with anti-OGG1 or anti-pro-SP-C antibodies (the control was AECII cells from untreated mice). Pulldown with Akt antibodies showed no association between OGG1 and pro-SP-C. (C) Reduction of DNA damage after PAO1 infection by overexpression of OGG1 in A549 cells with the retroviral vector ps91-EGFP-OGG1. Cells were infected with PAO1 for 1 h, and a comet assay was used to measure the extent of DNA damage versus that in vector control cells (**, $P < 0.01$). (D) Protection against PAO1 infection by overexpression of OGG1 in A549 cells versus vector control cells. Proliferation of infected cells (1 h of infection and ensuing incubation without bacteria for 48 h) was determined by MTT assay, and data are expressed as percentages (*, $P < 0.05$). The data shown are representative of three experiments.

oxidative damage, we attempted to identify the main cell type involved in *P. aeruginosa* infection in mice. By immunohistochemical analysis, OGG1 (red) was colocalized with AECII cells, as identified by pro-SP-C antibodies (green). In addition, OGG1 expression was increased (approximately 2.8-fold) compared to that in untreated controls, as determined by ImageJ software (Fig. 3A). In contrast, SP-C expression was not altered by infection. Furthermore, the ExoS-deficient strain could not induce OGG1 expression versus WT PAO1. These observations indicate that AECII cells may suffer from DNA damage and began to undergo a repair process following infection, consistent with previous findings in which AECII cells succumbed to hyperoxia-induced DNA damage (33, 79). To validate the cell type involved in the OGG1 response, we performed a pulldown of lung lysates with pro-SP-C antibodies and probed them with OGG1. Our data showed that AECII cells expressed high levels of OGG1 after infection (Fig. 3B), indicating that AECII cells play a critical role in repairing infection-induced DNA damage. In addition, OGG1 may be associated with pro-SP-C, as demonstrated by coimmunoprecipitation. In contrast, Akt was examined for comparison and was shown to have no association with pro-SP-C. It should be noted that the OGG1 antibodies cannot distinguish nuclear OGG1a from mitochondrial OGG1b and -c and OGG2 isoforms. Thus, OGG isoforms in cytosol may contribute to a part or all of the interaction with pro-SP-C.

OGG1 overexpression contributes to counteraction of *P. aeruginosa* infection. The above observations logically suggest that overexpression of OGG1 may increase host resistance to *P. aeruginosa*. To test this hypothesis, we transduced A549 cells with a retroviral construct containing full-length OGG1 (pSF91-OGG1) (20, 79). After the viral vector transduction, approximately 30 to 40% of cells expressed enhanced GFP (EGFP)-OGG1 initially, but we found that almost 100% of the populations expressed EGFP-OGG1 after selection by a flow cytometry sorter (data not shown). OGG1 expression was more than 100 times greater in pSF91-OGG1-transduced A549 cells than in vector controls, as assessed by Northern blotting, RT-PCR, and enzymatic activity assays as described previously (79). Additionally, our results show that overexpression of OGG1 significantly attenuated infection-induced DNA damage (reduced DNA strand breaks) compared to vector controls (Fig. 3C). After exposure to PAO1 for 1 h, the average comet tail length of cells overexpressing OGG1 was 5.75 ± 0.2 μm, while significantly longer tail lengths (19.5 ± 2.3 μm, $P < 0.05$) were found in vector-transduced cells. Further, the MTT assay

was utilized to determine cell proliferation rates (1 h infection and culturing in antibiotic medium for an additional 48 h), and our results showed that overexpression of OGG1 significantly reduced the rate of cell death compared to that in vector control cells (Fig. 3D, $P < 0.05$). Altogether, A549 cells overexpressing OGG1 exhibited stronger tolerance of PAO1 toxicity than did control cells.

Extensive DNA repair responses to *P. aeruginosa* infection. Recent studies suggest that multiple DNA repair proteins cooperatively initiate a global repair response during severe oxidative DNA damage (68). Because APE1, another crucial redox enzyme, is potentially activated following other Gram-negative infections (11), we investigated the APE1-mediated response to *P. aeruginosa*. CSB is a NER protein that has been linked to oxidation-induced DNA repair. Thus, we began to investigate several additional DNA repair proteins for roles in the response to PAO1 infection. Our results show that various PAO1 components induced differential responses by DNA repair proteins, including OGG1, CSB, and APE1 (Fig. 4A). The infection time was 4 h, but additional times tested showed similar induction patterns by DNA repair responses (data not shown). The induction of DNA repair activity appeared to be dependent on both the length and the concentration of bacterial exposure (data not shown). LPS, dead PAO1, and live PAO1 all induced the expression of DNA repair proteins. Because live PAO1 bacteria induced higher levels of APE1 and CSB expression, these two repair proteins may significantly contribute to the *in vivo* host defense. We next analyzed the localization of DNA repair enzymes during infection. By extracting the nucleus and cytosol, we tracked the compartmental shift of DNA repair proteins and found that PAO1 infection induced an increase in CSB expression in the nucleus. In contrast, the levels of the XPB and XRCC1 proteins in nuclei did not change. In the cytoplasm, an opposite dynamic takes place, with CSB expression decreased and XPB expression increased (Fig. 4B). To ensure that the isolation is valid, a nuclear marker (histone 1) and a cytosol marker (tubulin) were used to probe the proteins in nuclear and cytosolic fractions and whole lysates. These results suggest that CSB crosses the nuclear membrane to coordinate DNA repair activity by interacting with OGG1.

The expression of various DNA repair proteins was verified in WT C57BL/6 mice by immunochemical analysis, where no-infection controls showed no increase in the expression of either OGG1 (green) or XRCC1 (red) (Fig. 4C). However, PAO1 infection induced an increase in both OGG1 and XRCC1 (approximately 3.9-fold for each) in the lung, as measured by immunofluorescence assay (Fig. 4C). To further dissect OGG1's role in the response to bacterial infection, we studied whether acetylation sites of OGG1 are involved. Acetylation of OGG1 was previously revealed to enhance the glycosylase activity of the protein during oxidation, indicating that acetylation plays a role in regulating the function of OGG1 (5). To further define the role of OGG1 in bacterial infection, we transfected A549 cells with an OGG1 acetylation site mutant (OGG1-K338R/K341R) plasmid, which altered OGG1 staining versus controls (data not shown). Interestingly, infection with PAO1 led to a 4.4-fold increase in CSB expression (TRITC) compared to that in controls (Fig. 4D), indicating that CSB may compensate for the loss of OGG1 activity. OGG1 was colocalized with oxoG (FITC), suggesting a specific repair response to PAO1-induced DNA damage. Collectively, our data indicate that acetylation of OGG1 may increase OGG1 glycosylase activity during bacterial infection, consistent with the previously reported results obtained under oxidation conditions (5).

Interactions of DNA repair proteins during *P. aeruginosa* infection. To confirm the role of OGG1 acetylation, we assayed for OGG1 activity after mutating acetylation sites (K338R/K341R). Transfection with a plasmid with acetylation defects at these sites inhibited the induction of OGG1 following bacterial infection (Fig. 5A), suggesting that acetylation of OGG1 may indeed enhance OGG1 glycosylase activity. We did not see significant adverse effects due to transfection. The data also indicate that OGG1 acetylation may be associated with the host defense against PAO1. In contrast, XPB expression was not altered when OGG1 acetylation sites were mutated through transfection (Fig. 5B). Altogether, these data indicate that OGG1 acetylation enables upregulation of OGG1 activity, which may be associated with CSB but not with XPB.

Roles of OGG1 in lung cell death and tissue injury. Since OGG1 was implicated in the response to bacterial invasion, it is important to further study the role of OGG1 in the host defense. Using pooled siRNAs to knock down OGG1 in A549 cells, we demonstrated a 76% reduction in OGG1 expression by Western blotting (Fig. 5C). This reduction of OGG1 corresponded with an increase in DNA damage due to PAO1 infection. Using a trypan blue exclusion assay, we noticed greater cytotoxicity in OGG1 siRNA-transfected cells than in control cells (Fig. 5D), suggesting that OGG1 may play a key role in counteracting bacterium-induced cytotoxic effects.

To ascertain the beneficial role of OGG1 in PAO1 infection, we used $OGG1^{-/-}$ mice, which are currently the best available model for elucidating OGG1 function and physiological significance. To our pleasant surprise, $OGG1^{-/-}$ mice showed a reduced response (indicated by its expression) by CSB compared to $OGG1^{+/+}$ mice (Fig. 5E). The expression of PARP1 in $OGG1^{-/-}$ mice is slightly increased by infection compared to that in $OGG1^{-/-}$ mice (Fig. 5E), although $OGG1^{-/-}$ mice without infection had a lower level of PARP1 than did $OGG1^{+/+}$ mice. This result is consistent with the above findings, indicating that OGG1 plays a role in coordinating CSB function. To further understand the role of OGG1 in combating oxidation-inflammation and tissue injury, we examined the quantity of oxoG in $OGG1^{-/-}$ mice following PAO1 infection and found a significant oxoG increase (red) in the lungs versus those of the WT control, which was accompanied by an increased expression of interleukin-1β (IL-1β) (2.4-fold, FITC) in $OGG1^{-/-}$ mice compared to that in $OGG1^{+/+}$ mice (Fig. 6A). Notably, control groups without infection did not show apparent IL-1β expression. These results illustrate that oxidative DNA damage in $OGG1^{-/-}$ mice is more severe and results in significantly greater bacterial burdens than in WT mice (Fig. 6B). Additionally, PAO1 infection caused significant pathophysiological alterations, as shown by lung H&E staining, versus the control mice (Fig. 6C). Furthermore, PAO1 infection caused significant MPO production in $OGG1^{-/-}$ mice compared to $OGG1^{+/+}$ mice ($P < 0.01$, Fig. 6D), a strong

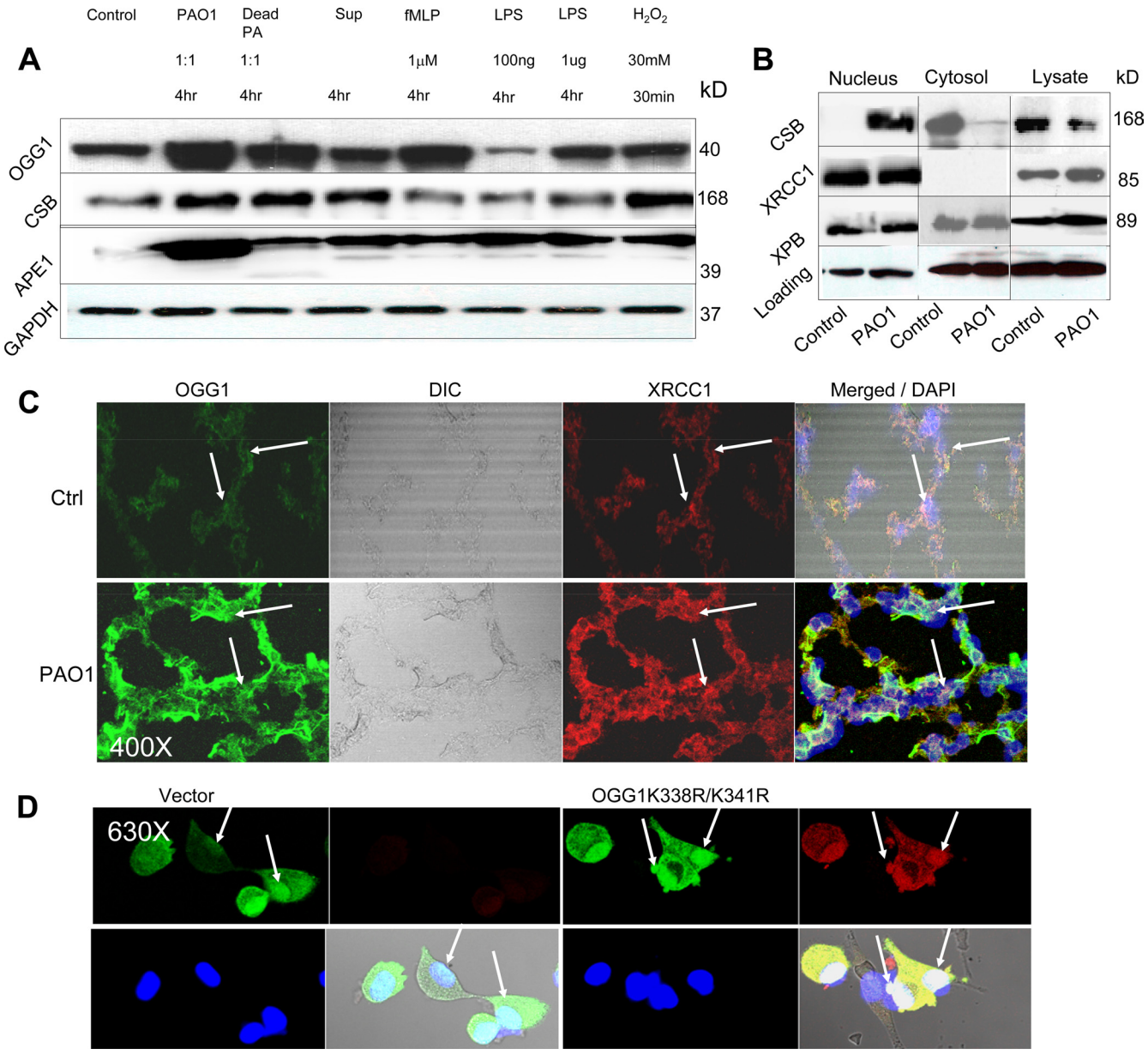

FIG. 4. Distinct responses to PAO1 by DNA repair proteins. (A) Induction of DNA repair proteins in lung cells by various PAO1 components. Components or bacteria were used as described in the legend to Fig. 1D (Sup, PAO1 culture supernatant). After infection, A549 cell lysates were probed with antibodies against various DNA repair proteins as indicated. The data shown are for 4 h of PAO1 infection. Additional infection times (1 h and 18 h) were examined, and similar results (not shown) were obtained. (B) Compartmental distribution of DNA repair proteins following PAO1 infection of A549 cells determined by Western blotting. The nucleus and cytoplasm of lung cells were isolated by multiple centrifugations (see Materials and Methods). (C) Induction of OGG1 and XRCC1 expression in the lung (colocalization) as shown by immunofluorescence assay after intranasal instillation of PAO1 for 18 h. After lavage to remove the free bacteria, the lungs were fixed with OCT and stained with antibodies as indicated. The no-infection control showed much less staining. DIC, differential interference contrast. (D) Increased CSB expression in A549 cells through perturbation of OGG1 acetylation by transfecting an OGG1-K338R/K341R construct. Colocalization between CSB (TRITC) and oxoG (FITC) is indicated (pink and purple). The vector-only control shows less staining. The data shown are representative of three experiments.

indicator of lung injury. PAO1 infection also inflicted statistically significantly stronger lipid peroxidation in $OGG1^{-/-}$ mice than in $OGG1^{+/+}$ mice ($P < 0.01$, Fig. 6E). Finally, oxidative DNA damage by PAO1 infection resulted in more severe lung injury in $OGG1^{-/-}$ mice, as manifested by a statistically significant increase in wet/dry ratios compared to those of $OGG1^{+/+}$ mice (Fig. 6F). Similarly, albumin in the bronchoalveolar lavage fluid was also increased after infection (data not shown). Taken together, our data strongly indicate that OGG1 is crucial in reducing various toxic effects caused by PAO1 infection.

In summary, we have identified a novel DNA repair response to *P. aeruginosa* infection. The bacterium induces significant DNA damage, which initiates a broad range of DNA

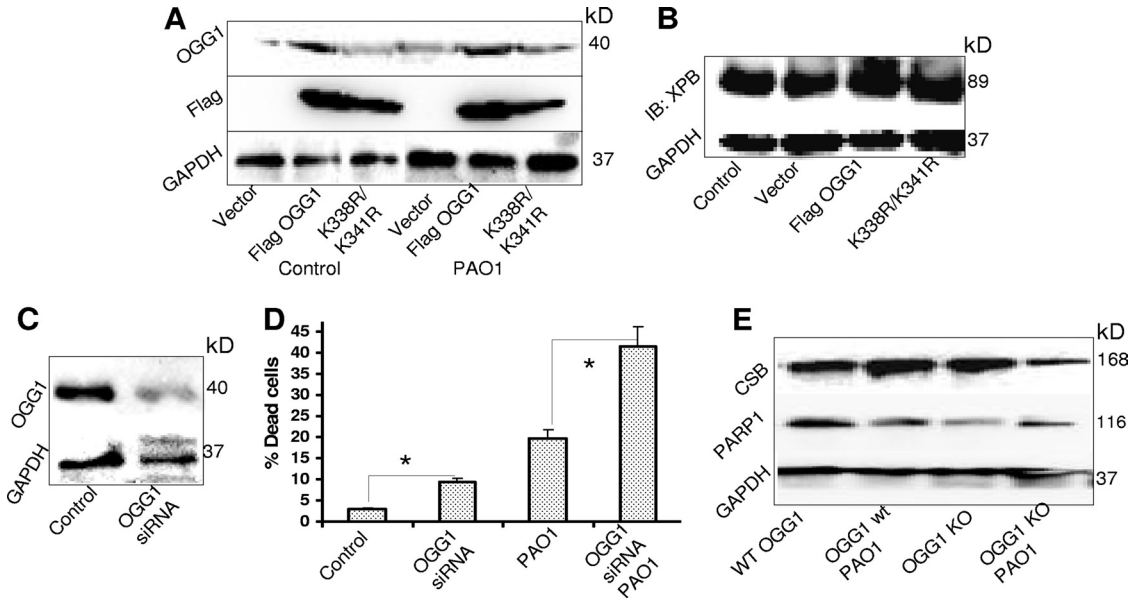

FIG. 5. Interaction of DNA repair proteins in response to PAO1 infection. (A) Perturbation of OGG1 acetylation reduced the DNA repair response to infectious oxidation. A549 cells were transfected with a mutant FLAG-OGG1 construct with defects in acetylation sites (K338R/K341R) or with a WT FLAG-OGG1 construct. The lysates were probed with either OGG1 or FLAG antibodies. Sample loading was monitored by GAPDH. (B) Expression of XPB and OGG1 after perturbation of OGG1 acetylation sites. Cell lysates were probed with XPB and GAPDH (loading) antibodies, respectively. IB, immunoblotting. (C) Transfection of OGG1 siRNA decreased the expression of OGG1 in AECII cells. The expression of OGG1 was measured by Western blotting with antibodies against OGG1 and reprobed with GAPDH (loading control). (D) Transfection of OGG1 siRNA decreased AECII cell survival compared to that of controls (trypan blue exclusion; *, $P < 0.05$). (E) Loss of OGG1 reduced responses to bacterial infection by CSB and PARP1 in OGG1$^{-/-}$ mice versus OGG1$^{+/+}$ mice (five mice per group). Lung lysates were assessed for DNA repair protein expression as indicated (Western blotting). The data shown are representative of three experiments.

repair responses. The chief responder is the BER pathway and is initiated by OGG1. In addition, a significant response may require the participation of other DNA repair proteins such as CSB and XPB (Fig. 7).

DISCUSSION

Limited studies have investigated DNA repair functions in response to Gram-negative bacteria such as *H. pylori* (11), while no research has examined the DNA damage response to *P. aeruginosa*. Our current study demonstrates that *P. aeruginosa* infection causes severe DNA damage, which subsequently activates a group of DNA repair proteins (OGG1, APE1, and CSB). These responses are crucial for homeostasis during bacterial infection (60). Bacterium-induced cell death is classified into three modes: pyroptosis, necrosis, and apoptosis (4). However, the dominant pathway involved in bacterial infection may be pyroptosis (caspase 1-dependent cell death). These fatal outcomes for host cells have previously been shown to contribute to lung pathology (1, 7, 28, 32). Apoptotic cell death or pyroptosis, if not efficiently counteracted by DNA repair systems, can lead to acute lung injury (50, 53).

Numerous virulent components of *P. aeruginosa* can induce lung cell death, including type IV pili, which play an important role in twitching activity, and the T3SS (86). Furthermore, pilus-deficient mutants have been shown to display a decreased ability to adhere to and invade alveolar epithelial cells (9). Infection with bacteria elicits a massive inflammatory response, which is a key pathogenic process that is primarily regulated by cytokines and chemokines such as IL-1β, IL-6, IL-8 (KC in mice), IL-12, and TNF-α (35, 36, 47, 73). Dysregulated inflammatory responses may trigger an excessive ROS release that damages host genomic DNA and subsequently induces DNA repair responses. We hypothesized that *P. aeruginosa*-induced DNA damage may directly contribute to pathogenesis. Our studies demonstrate that PAO1 causes a commonly induced DNA damage adduct—oxoG. This DNA damage may induce cell cycle arrest and ultimately cell death. Intensive cell death leads to tissue injury, organ failure, and eventual death.

We also examined a host defense role of DNA repair proteins in lung epithelial cells. DNA repair proteins may directly respond to and repair DNA damage, thereby alleviating tissue injury. As expected, we found that DNA repair responses are indeed initiated to counteract bacterial infection, which may play a role in lessening inflammatory responses and tissue injury. When these repair processes are perturbed, host homeostasis can be severely impaired, leading to increased tissue injury. To further test this hypothesis, we used siRNA to downregulate OGG1 and showed that OGG1 reduction promotes accumulation of DNA damage, resulting in less cell survival. The DNA repair activity of OGG1 seems to be dependent at least partially on its acetylation sites, as perturbing these sites also hampered the interaction of OGG1 with CSB, which may increase DNA damage and reduce cell viability. In contrast, overexpression of OGG1 by a retroviral vector protected lung cells from bacterium-induced DNA damage, increasing cell survival. Hence, OGG1 seems to benefit the host by reducing bacterium-induced toxicity.

To effectively repair oxidative DNA damage, DNA repair

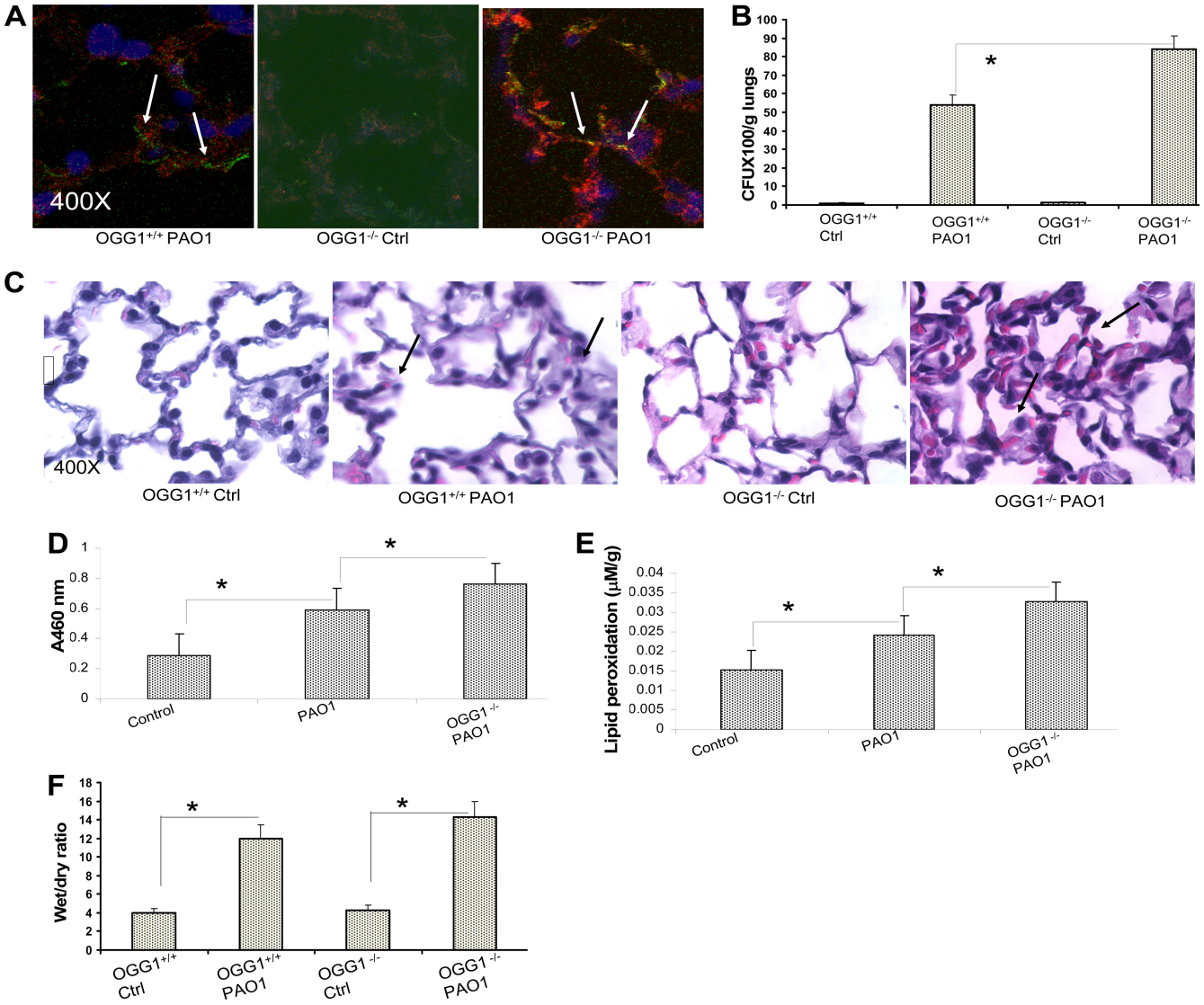

FIG. 6. Exacerbation of lung injury due to infection in OGG1$^{-/-}$ mice versus OGG1$^{+/+}$ mice. (A) Increased IL-1β is associated with DNA damage in OGG1$^{-/-}$ mice compared to OGG1$^{+/+}$ mice. Mice were infected intranasally with PAO1 for 1 day. Immunohistochemical analysis was performed with IL-1β antibodies (TRITC) and oxoG antibodies (FITC). Arrows show colocalization sites. The noninfected control (Ctrl) showed nearly no staining (five mice per KO or WT group). (B) Increased bacterial burdens in OGG1$^{-/-}$ mice compared to those in OGG1$^{+/+}$ mice. Following 1 day of infection with PAO1, CFU were numerated in homogenized lung lysates. (C) Increased lung injury in OGG1$^{-/-}$ mice compared to that in OGG1$^{+/+}$ mice as determined by histology analysis. Infection was performed by intranasal PAO1 instillation for 1 day. The samples were processed by paraffin sectioning and stained by a routine H&E staining method (*, $P < 0.05$). Arrows show the sites with strong inflammatory responses. (D) PAO1 infection induced significant MPO production in OGG1$^{-/-}$ mice compared to OGG1$^{+/+}$ mice (*, $P < 0.05$). After 1 day of infection, MPO was measured in homogenized lung lysates. Control, OGG1$^{+/+}$ mice with no bacteria; PAO1, PAO1-infected OGG1$^{+/+}$ mice; OGG1$^{-/-}$, PAO1-infected OGG1$^{-/-}$ mice. (E) PAO1 infection induced more lipid peroxidation in OGG1$^{-/-}$ mice than in OGG1$^{+/+}$ mice (*, $P < 0.05$). Following 1 day of PAO1 infection, homogenized lung lysates were assayed by the malondialdehyde method. Control, OGG1$^{+/+}$ mice with no bacteria; PAO1, PAO1-infected OGG1$^{+/+}$ mice; OGG1$^{-/-}$, PAO1-infected OGG1$^{-/-}$ mice. (F) Increase in the wet/dry ratio in OGG1$^{-/-}$ mice compared to that in OGG1$^{+/+}$ mice (*, $P < 0.05$). The data shown are representative of three experiments.

proteins may interact with other signaling proteins, such as transcriptional factors or protein kinases (33, 50), controlling the expression and secretion of cytokines (26). This multifaceted determination of host cell fate is the case during *P. aeruginosa* infection. Since previous studies have indicated the involvement of kinases in apoptotic responses to *P. aeruginosa* (27) and to hyperoxia (12), we propose that various cellular signaling pathways may enhance the BER pathway function to alleviate oxidative DNA damage. We further demonstrated that nuclear excision DNA repair proteins such as CSB, a crucial gene product for Cockayne syndrome, may be critical to the host defense against *P. aeruginosa*. Previous studies have shown that CSB may be required for removal of oxoG and repair of the DNA damage (72), but the exact role and process are undefined. To begin to delineate this molecular mechanism, we demonstrate that reduction of OGG1's acetylation ability increased the expression of CSB, suggesting that CSB may compensate for the loss of OGG1's glycosylase activity.

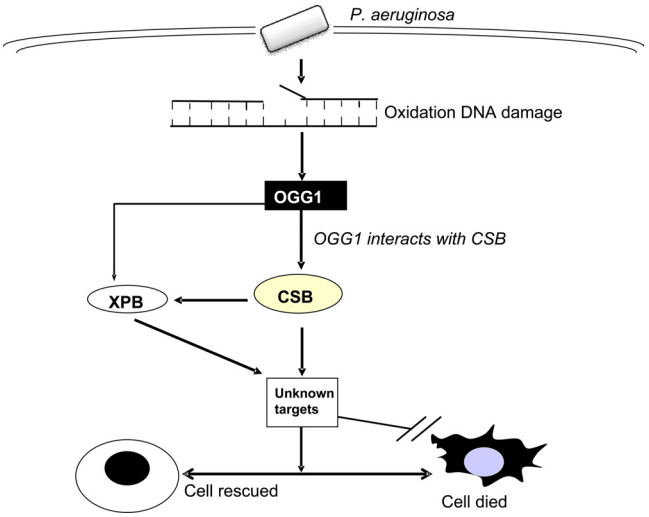

FIG. 7. Schematic representation of the DNA repair response after *P. aeruginosa* infection. The bacterium causes significant DNA damage, which in turn initiates a broad range of DNA repair responses. OGG1 is a main responder and interacts with CSB, as well as XPB. This response may also involve other signals, such as Akt and ERK1/2 (not shown), to counteract DNA damage and rescue injured cells.

The activity of OGG1 may be linked to the bacterial pathogenic factor ExoS since ExoS deficiency induced much-reduced OGG1 expression (Fig. 2B). Furthermore, XRCC1 (a scaffold protein for the BER pathway) (43) can recruit DNA repair proteins through interaction with CSB. XRCC1 may also counteract an excessive inflammatory response by downregulating PARP1 activity (3). PARP1, a scaffold protein and inflammatory factor, is significantly upregulated in response to *P. aeruginosa* infection. Previous studies show that PARP1 expression can be decreased by XRCC1 through its BRCA-1 C-terminal domain (32). We showed that PARP1 can be shut down in OGG1 KO mice, suggesting that OGG1 is involved in inflammatory responses. Although a more detailed understanding is needed, our results already suggest that DNA repair proteins play a role in the balance between fighting bacterial infection and triggering potentially dangerous inflammatory conditions.

We also attempted to identify the components of the bacterium that are responsible for inducing DNA repair responses. Exoenzymes (T3SS) have been shown to be significant in inducing cellular signaling pathways. Our data showed that ExoS played typical roles in initiating OGG1. Previously, ExoS was reported to interfere with the ERM proteins by its ADP ribosylation and GTPase activity (42), thereby preventing the activation of key regulators of actin nucleation. Thus, induction of OGG1 by ExoS may be associated with its ADP ribosylation activity. Interestingly, ExoS may have a dual role in regulating caspase 1-mediated IL-1β maturation (14). However, the exact mechanism of this function is still unknown and warrants further study.

Finally, we investigated the pathophysiological significance of the OGG1 DNA repair response using OGG1 KO mice. These mice showed intensified lung injury compared to WT mice following *P. aeruginosa* infection, suggesting that OGG1 is involved in the host response to pathogen-induced oxidation. These data also indicate that inflammatory responses can be upregulated (due to loss of OGG1) and contribute to acute lung injury.

Using both *in vitro* and *in vivo* models, our studies have revealed a novel dimension of the host defense, i.e., that the BER pathway is involved in *P. aeruginosa* infection in lung epithelial cells. This potential new role for DNA repair proteins as an immunoregulatory factor may be of general significance for the host defense against Gram-negative bacteria, particularly in immunodeficient individuals. One of the important questions that may arise from our results is whether genotoxicity and the OGG1-associated response are bacterium specific. Various DNA repair responses could be induced by other bacteria, for instance, as in the finding by Ding et al. that *H. pylori* induced digestive epithelial cells to express higher levels of the DNA repair protein APE1 (11). Similarly, our pilot study suggests that another respiratory pathogen, *Klebsiella pneumoniae*, can induce DNA damage and a subsequent DNA repair response (unpublished data). Although some questions remain to be answered, the present study demonstrates that a respiratory bacterium induces DNA damage and a DNA repair response in the lung. We also show that an attenuated PAO1 strain (ΔExoS) induces less severe DNA damage. Using OGG1 KO mice, we have systematically dissected and ascertained the aforementioned novel mechanism—the BER pathway is critically involved in the host defense against Gram-negative infection of the lung.

It is challenging to formally establish the physiological relevance of OGG1 in infectious diseases and delineate the underlying molecular mechanism. Since host neutrophils and macrophages can also release excessive ROS or indirectly produce oxidants, it is important to differentiate the oxidation effects caused by the bacterium from those caused by the host. In conclusion, our study demonstrates a novel response to *P. aeruginosa* by the host DNA repair system, which suggests novel therapeutics for treating this refractory infection and for other Gram-negative pathogen infections.

ACKNOWLEDGMENTS

This work was supported by NIH ES014690 and an American Heart Association Scientist Development Grant (National Office). This work was also supported by the National Key Basic Research Program of China (973Program 2006CB504300).

We thank Gerald Pier and Joseph T. Barbieri for providing various PA strains. We thank S. Rolling of the University of North Dakota imaging core for help with confocal imaging. We also thank Lushen Wu of Harvard University for reading the manuscript.

We have no competing financial interests.

REFERENCES

1. **Alaoui-El-Azher, M., J. Jia, W. Lian, and S. Jin.** 2006. ExoS of Pseudomonas aeruginosa induces apoptosis through a Fas receptor/caspase 8-independent pathway in HeLa cells. Cell. Microbiol. **8:**326–338.
2. **Barker, G. F., N. D. Manzo, K. L. Cotich, R. K. Shone, and A. B. Waxman.** 2006. DNA damage induced by hyperoxia: quantitation and correlation with lung injury. Am. J. Respir. Cell Mol. Biol. **35:**277–288.
3. **Beernink, P. T., M. Hwang, M. Ramirez, M. B. Murphy, S. A. Doyle, and M. P. Thelen.** 2005. Specificity of protein interactions mediated by BRCT domains of the XRCC1 DNA repair protein. J. Biol. Chem. **280:**30206–30213.
4. **Bergsbaken, T., S. L. Fink, and B. T. Cookson.** 2009. Pyroptosis: host cell death and inflammation. Nat. Rev. Microbiol. **7:**99–109.
5. **Bhakat, K. K., S. K. Mokkapati, I. Boldogh, T. K. Hazra, and S. Mitra.** 2006. Acetylation of human 8-oxoguanine-DNA glycosylase by p300 and its role in 8-oxoguanine repair in vivo. Mol. Cell. Biol. **26:**1654–1665.
6. **Burns, J. L., R. L. Gibson, S. McNamara, D. Yim, J. Emerson, M. Rosenfeld, P. Hiatt, K. McCoy, R. Castile, A. L. Smith, and B. W. Ramsey.** 2001.

Longitudinal assessment of Pseudomonas aeruginosa in young children with cystic fibrosis. J. Infect. Dis. **183:**444–452.
7. **Cannon, C. L., M. P. Kowalski, K. S. Stopak, and G. B. Pier.** 2003. Pseudomonas aeruginosa-induced apoptosis is defective in respiratory epithelial cells expressing mutant cystic fibrosis transmembrane conductance regulator. Am. J. Respir. Cell Mol. Biol. **29:**188–197.
8. **Cheng, K. C., D. S. Cahill, H. Kasai, S. Nishimura, and L. A. Loeb.** 1992. 8-Hydroxyguanine, an abundant form of oxidative DNA damage, causes G—-T and A—-C substitutions. J. Biol. Chem. **267:**166–172.
9. **Comolli, J. C., L. L. Waite, K. E. Mostov, and J. N. Engel.** 1999. Pili binding to asialo-GM1 on epithelial cells can mediate cytotoxicity or bacterial internalization by *Pseudomonas aeruginosa*. Infect. Immun. **67:**3207–3214.
10. **Davies, G. R., N. J. Simmonds, T. R. Stevens, M. T. Sheaff, N. Banatvala, I. F. Laurenson, D. R. Blake, and D. S. Rampton.** 1994. Helicobacter pylori stimulates antral mucosal reactive oxygen metabolite production in vivo. Gut **35:**179–185.
11. **Ding, S. Z., A. M. O'Hara, T. L. Denning, B. Dirden-Kramer, R. C. Mifflin, V. E. Reyes, K. A. Ryan, S. N. Elliott, T. Izumi, I. Boldogh, S. Mitra, P. B. Ernst, and S. E. Crowe.** 2004. Helicobacter pylori and H2O2 increase AP endonuclease-1/redox factor-1 expression in human gastric epithelial cells. Gastroenterology **127:**845–858.
12. **Epelman, S., B. Berenger, D. Stack, G. G. Neely, L. L. Ma, and C. H. Mody.** 2008. Microbial products activate monocytic cells through detergent-resistant membrane microdomains. Am. J. Respir. Cell Mol. Biol. **39:**657–665.
13. **Farinati, F., R. Cardin, P. Degan, M. Rugge, F. D. Mario, P. Bonvicini, and R. Naccarato.** 1998. Oxidative DNA damage accumulation in gastric carcinogenesis. Gut **42:**351–356.
14. **Galle, M., P. Schotte, M. Haegman, A. Wullaert, H. J. Yang, S. Jin, and R. Beyaert.** 2008. The Pseudomonas aeruginosa type III secretion system plays a dual role in the regulation of caspase-1 mediated IL-1beta maturation. J. Cell Mol. Med. **12:**1767–1776.
15. **Grassmé, H., S. Kirschnek, J. Riethmueller, A. Riehle, G. von Kurthy, F. Lang, M. Weller, and E. Gulbins.** 2000. CD95/CD95 ligand interactions on epithelial cells in host defense to Pseudomonas aeruginosa. Science **290:**527–530.
16. **Grollman, A. P., and M. Moriya.** 1993. Mutagenesis by 8-oxoguanine: an enemy within. Trends Genet. **9:**246–249.
17. **Hayden, P. J., P. Tewari, D. W. Morris, A. Staines, D. Crowley, A. Nieters, N. Becker, S. de Sanjosé, L. Foretova, M. Maynadié, P. L. Cocco, P. Boffetta, P. Brennan, S. J. Chanock, P. V. Browne, and M. Lawler.** 2007. Variation in DNA repair genes XRCC3, XRCC4, XRCC5 and susceptibility to myeloma. Hum. Mol. Genet. **16:**3117–3127.
18. **Hazra, T. K., J. W. Hill, T. Izumi, and S. Mitra.** 2001. Multiple DNA glycosylases for repair of 8-oxoguanine and their potential *in vivo* functions. Prog. Nucleic Acid Res. Mol. Biol. **68:**193–205.
19. **He, Y., M. Wu, Y. Kobune, Y. Xu, M. R. Kelley, and W. J. Martin II.** 2001. Expression of yeast apurinic/apyrimidinic endonuclease (APN1) protects lung epithelial cells from bleomycin toxicity. Am. J. Respir. Cell. Mol. Biol. **25:**692–698.
20. **He, Y., Y. Xu, M. Wu, M. Kobune, M. R. Kelley, and W. J. Martin II.** 2002. *Escherichia coli* FPG and human Ogg1 reduce DNA damage and cytotoxicity by BCNU in human lung cells. Am. J. Physiol. Lung Cell. Mol. Physiol. **182:**L50–L55.
21. **Hegde, M. L., T. K. Hazra, and S. Mitra.** 2008. Early steps in the DNA base excision/single-strand interruption repair pathway in mammalian cells. Cell Res. **18:**27–47.
22. **Heijerman, H.** 2005. Infection and inflammation in cystic fibrosis: a short review. J. Cyst. Fibros. **4**(Suppl. 2)**:**3–5.
23. **Hotchkiss, R. S., W. M. Dunne, P. E. Swanson, C. G. Davis, K. W. Tinsley, K. C. Chang, T. G. Buchman, and I. E. Karl.** 2001. Role of apoptosis in Pseudomonas aeruginosa pneumonia. Science **294:**1783.
24. **Hu, J., S. Z. Imam, K. Hashiguchi, N. C. de Souza-Pinto, and V. A. Bohr.** 2005. Phosphorylation of human oxoguanine DNA glycosylase (alpha-OGG1) modulates its function. Nucleic Acids Res. **33:**3271–3282.
25. **Izumi, T., L. R. Wiederhold, G. Roy, R. Roy, A. Jaiswal, K. K. Bhakat, and S. Mitra.** 2003. Mammalian DNA base excision repair proteins: their interactions and role in repair of oxidative DNA damage. Toxicology **193:**43–65.
26. **Jaiswal, M., N. F. LaRusso, L. J. Burgart, and G. J. Gores.** 2000. Inflammatory cytokines induce DNA damage and inhibit DNA repair in cholangiocarcinoma cells by a nitric oxide-dependent mechanism. Cancer Res. **60:**184–190.
27. **Jendrossek, V., H. Grassmé, I. Mueller, F. Lang, and E. Gulbins.** 2001. *Pseudomonas aeruginosa*-induced apoptosis involves mitochondria and stress-activated protein kinases. Infect. Immun. **69:**2675–2683.
28. **Jenkins, C. E., A. Swiatoniowski, A. C. Issekutz, and T. J. Lin.** 2004. Pseudomonas aeruginosa exotoxin A induces human mast cell apoptosis by a caspase-8 and -3-dependent mechanism. J. Biol. Chem. **279:**37201–37207.
29. **Jin, Y., S. Kannan, M. Wu, and J. X. Zhao.** 2007. Toxicity of luminescent silica nanoparticles to living cells. Chem. Res. Toxicol. **20:**1126–1133.
30. **Kannan, K., H. Huang, D. Seeger, A. Audet, Y. Chen, C. Huang, H. Gao, S. Li, and M. Wu.** 2009. Alveolar epithelial type II cells activate alveolar macrophages and mitigate P. aeruginosa infection. PLoS One **4:**e4891.
31. **Kannan, S., A. Audet, H. Huang, L. J. Chen, and M. Wu.** 2008. Cholesterol-rich membrane rafts and Lyn are involved in phagocytosis during Pseudomonas aeruginosa infection. J. Immunol. **180:**2396–2408.
32. **Kannan, S., A. Audet, J. Knittel, S. Mullegama, G. F. Gao, and M. Wu.** 2006. Src kinase Lyn is crucial for Pseudomonas aeruginosa internalization into lung cells. Eur. J. Immunol. **36:**1739–1752.
33. **Kannan, S., H. Pang, D. Foster, Z. Rao, and M. Wu.** 2006. Human 8-oxoguanine DNA glycosylase links MAPK activation to resistance to hyperoxia in lung epithelial cells. Cell Death Differ. **13:**311–323.
34. **Kim, J. J., H. Tao, E. Carloni, W. K. Leung, D. Y. Graham, and A. R. Sepulveda.** 2002. Helicobacter pylori impairs DNA mismatch repair in gastric epithelial cells. Gastroenterology **123:**542–553.
35. **Kooguchi, K., S. Hashimoto, A. Kobayashi, Y. Kitamura, I. Kudoh, J. Wiener-Kronish, and T. Sawa.** 1998. Role of alveolar macrophages in initiation and regulation of inflammation in *Pseudomonas aeruginosa* pneumonia. Infect. Immun. **66:**3164–3169.
36. **Kube, D., U. Sontich, D. Fletcher, and P. B. Davis.** 2001. Proinflammatory cytokine responses to P. aeruginosa infection in human airway epithelial cell lines. Am. J. Physiol. Lung Cell. Mol. Physiol. **280:**L493–L502.
37. **Lu, A. L., X. Li, Y. Gu, P. M. Wright, and D. Y. Chang.** 2001. Repair of oxidative DNA damage: mechanisms and functions. Cell Biochem. Biophys. **35:**141–170.
38. **Lucero, H., D. Gae, and G. E. Taccioli.** 2003. Novel localization of the DNA-PK complex in lipid rafts: a putative role in the signal transduction pathway of the ionizing radiation response. J. Biol. Chem. **278:**22136–22143.
39. **Mabley, J. G., P. Pacher, A. Deb, R. Wallace, R. H. Elder, and C. Szabo.** 2005. Potential role for 8-oxoguanine DNA glycosylase in regulating inflammation. FASEB J. **19:**290–292.
40. **Maiti, A. K., I. Boldogh, H. Spratt, S. Mitra, and T. K. Hazra.** 2008. Mutator phenotype of mammalian cells due to deficiency of NEIL1 DNA glycosylase, an oxidized base-specific repair enzyme. DNA Repair (Amsterdam) **7:**1213–1220.
41. **Mañes, S., G. del Real, and A. C. Martinez.** 2003. Pathogens: raft hijackers. Nat. Rev. Immunol. **3:**557–568.
42. **Maresso, A. W., M. R. Baldwin, and J. T. Barbieri.** 2004. Ezrin/radixin/moesin proteins are high affinity targets for ADP-ribosylation by Pseudomonas aeruginosa ExoS. J. Biol. Chem. **279:**38402–38408.
43. **Marsin, S., A. E. Vidal, M. Sossou, J. Menissier-de Murcia, F. Le Page, S. Boiteux, G. de Murcia, and J. P. Radicella.** 2003. Role of XRCC1 in the coordination and stimulation of oxidative DNA damage repair initiated by the DNA glycosylase hOGG1. J. Biol. Chem. **278:**44068–44074.
44. **Michiels, C., M. Raes, O. Toussaint, and J. Remacle.** 1994. Importance of Se-glutathione peroxidase, catalase, and Cu/Zn-SOD for cell survival against oxidative stress. Free Radic. Biol. Med. **17:**235–248.
45. **Mitra, S., I. Boldogh, T. Izumi, and T. K. Hazra.** 2001. Complexities of the DNA base excision repair pathway for repair of oxidative DNA damage. Environ. Mol. Mutagen. **38:**180–190.
46. **Morero, N. R., and C. E. Argaraña.** 2009. Pseudomonas aeruginosa deficient in 8-oxodeoxyguanine repair system shows a high frequency of resistance to ciprofloxacin. FEMS Microbiol. Lett. **290:**217–226.
47. **Murphey, E. D., D. N. Herndon, and E. R. Sherwood.** 2004. Gamma interferon does not enhance clearance of *Pseudomonas aeruginosa* but does amplify a proinflammatory response in a murine model of postseptic immunosuppression. Infect. Immun. **72:**6892–6901.
48. **Nardone, L. L., and S. B. Andrews.** 1979. Cell line A549 as a model of the type II pneumocyte. Phospholipid biosynthesis from native and organometallic precursors. Biochim. Biophys. Acta **573:**276–295.
49. **Nishimura, S.** 2001. Mammalian Ogg1/Mmh gene plays a major role in repair of the 8-hydroxyguanine lesion in DNA. Prog. Nucleic Acid Res. Mol. Biol. **68:**107–123.
50. **Offer, H., R. Wolkowicz, D. Matas, S. Blumenstein, Z. Livneh, and V. Rotter.** 1999. Direct involvement of p53 in the base excision repair pathway of the DNA repair machinery. FEBS Lett. **450:**197–204.
51. **Ohkawa, H., N. Ohishi, and K. Yagi.** 1979. Assay for lipid peroxides in animal tissues by thiobarbituric acid reaction. Anal. Biochem. **95:**351–358.
52. **O'Reilly, M. A., R. J. Staversky, R. H. Watkins, W. M. Maniscalco, and P. C. Keng.** 2000. p53-independent induction of GADD45 and GADD153 in mouse lungs exposed to hyperoxia. Am. J. Physiol. Lung Cell. Mol. Physiol. **278:**L552–L559.
53. **Panayiotidis, M. I., R. C. Rancourt, C. B. Allen, S. R. Riddle, B. K. Schneider, S. Ahmad, and C. W. White.** 2004. Hyperoxia-induced DNA damage causes decreased DNA methylation in human lung epithelial-like A549 cells. Antioxid. Redox Signal. **6:**129–136.
54. **Plotkowski, M. C., H. C. Povoa, J. M. Zahm, G. Lizard, G. M. Pereira, J. M. Tournier, and E. Puchelle.** 2002. Early mitochondrial dysfunction, superoxide anion production, and DNA degradation are associated with non-apoptotic death of human airway epithelial cells induced by Pseudomonas aeruginosa exotoxin A. Am. J. Respir. Cell Mol. Biol. **26:**617–626.
55. **Priebe, G. P., M. M. Brinig, K. Hatano, M. Grout, F. T. Coleman, G. B. Pier, and J. B. Goldberg.** 2002. Construction and characterization of a live, attenuated *aroA* deletion mutant of *Pseudomonas aeruginosa* as a candidate intranasal vaccine. Infect. Immun. **70:**1507–1517.

56. **Qin, L., X. Wu, M. L. Block, Y. Liu, G. R. Breese, J. S. Hong, D. J. Knapp, and F. T. Crews.** 2007. Systemic LPS causes chronic neuroinflammation and progressive neurodegeneration. Glia **55:**453–462.
57. **Rajan, S., G. Cacalano, R. Bryan, A. J. Ratner, C. U. Sontich, A. van Heerckeren, P. Davis, and A. Prince.** 2000. Pseudomonas aeruginosa induction of apoptosis in respiratory epithelial cells: analysis of the effects of cystic fibrosis transmembrane conductance regulator dysfunction and bacterial virulence factors. Am. J. Respir. Cell Mol. Biol. **23:**304–312.
58. **Richards, J. D., L. Cubeddu, J. Roberts, H. Liu, and M. F. White.** 2008. The archaeal XPB protein is a ssDNA-dependent ATPase with a novel partner. J. Mol. Biol. **376:**634–644.
59. **Richardson, A. R., K. C. Soliven, M. E. Castor, P. D. Barnes, S. J. Libby, and F. C. Fang.** 2009. The base excision repair system of Salmonella enterica serovar Typhimurium counteracts DNA damage by host nitric oxide. PLoS Pathog. **5:**e1000451.
60. **Rolseth, V., E. Rundén-Pran, L. Luna, C. McMurray, M. Bjørås, and O. P. Ottersen.** 2008. Widespread distribution of DNA glycosylases removing oxidative DNA lesions in human and rodent brains. DNA Repair (Amsterdam) **7:**1578–1588.
61. **Saliba, A. M., M. C. de Assis, R. Nishi, B. Raymond, E. A. Marques, U. G. Lopes, L. Touqui, and M. C. Plotkowski.** 2006. Implications of oxidative stress in the cytotoxicity of Pseudomonas aeruginosa ExoU. Microbes Infect. **8:**450–459.
62. **Schümann, J., H. Bluethmann, and G. Tiegs.** 2000. Synergism of Pseudomonas aeruginosa exotoxin A with endotoxin, superantigen, or TNF results in TNFR1- and TNFR2-dependent liver toxicity in mice. Immunol. Lett. **74:**165–172.
63. **Shibutani, S., M. Takeshita, and A. P. Grollman.** 1991. Insertion of specific bases during DNA synthesis past the oxidation-damaged base 8-oxodG. Nature **349:**431–434.
64. **Simons, K., and D. Toomre.** 2000. Lipid rafts and signal transduction. Nat. Rev. Mol. Cell Biol. **1:**31–39.
65. **Soong, G., D. Parker, M. Magargee, and A. S. Prince.** 2008. The type III toxins of *Pseudomonas aeruginosa* disrupt epithelial barrier function. J. Bacteriol. **190:**2814–2821.
66. **Spragg, R. G., and J. Li.** 2000. Effects of phosphocholine cytidylytransferase expression on phosphatidylcholine synthesis in alveolar type II cells and related cell lines. Am. J. Respir. Cell Mol. Biol. **22:**116–124.
67. **Sun, J., and J. T. Barbieri.** 2004. ExoS Rho GTPase-activating protein activity stimulates reorganization of the actin cytoskeleton through Rho GTPase guanine nucleotide disassociation inhibitor. J. Biol. Chem. **279:** 42936–42944.
68. **Sunesen, M., T. Stevnsner, R. M. J. Brosh, G. L. Dianov, and V. A. Bohr.** 2002. Global genome repair of 8-oxoG in hamster cells requires a functional CSB gene product. Oncogene **21:**3571–3578.
69. **Thorslund, T., C. von Kobbe, J. A. Harrigan, F. E. Indig, M. Christiansen, T. Stevnsner, and V. A. Bohr.** 2005. Cooperation of the Cockayne syndrome group B protein and poly(ADP-ribose) polymerase 1 in the response to oxidative stress. Mol. Cell. Biol. **25:**7625–7636.
70. **Tice, R. R., E. Agurell, D. Anderson, B. Burlinson, A. Hartmann, H. Kobayashi, Y. Miyamae, E. Rojas, J. C. Ryu, and Y. F. Sasaki.** 2000. Single cell gel/comet assay: guidelines for in vitro and in vivo genetic toxicology testing. Environ. Mol. Mutagen. **35:**206–221.
71. **Tuo, J., C. Chen, X. Zeng, M. Christiansen, and V. A. Bohr.** 2002. Functional crosstalk between hOgg1 and the helicase domain of Cockayne syndrome group B protein. DNA Repair (Amsterdam) **1:**913–927.
72. **Tuo, J., P. Jaruga, H. Rodriguez, M. Dizdaroglu, and V. A. Bohr.** 2002. The Cockayne syndrome group B gene product is involved in cellular repair of 8-hydroxyadenine in DNA. J. Biol. Chem. **277:**30832–30837.
73. **Voynow, J. A., S. J. Gendler, and M. C. Rose.** 2006. Regulation of mucin genes in chronic inflammatory airway diseases. Am. J. Respir. Cell Mol. Biol. **34:**661–665.
74. **Watanabe, N., D. A. Dickinson, D. M. Krzywanski, K. E. Iles, H. Zhang, C. J. Venglarik, and H. J. Forman.** 2002. A549 subclones demonstrate heterogeneity in toxicological sensitivity and antioxidant profile. Am. J. Physiol. Lung Cell. Mol. Physiol. **283:**L726–L736.
75. **Wu, M.** 2005. DNA repair proteins as molecular therapeutics for oxidative and alkylating lung injury. Curr. Gene Ther. **5:**225–236.
76. **Wu, M., A. Audet, J. Cusic, D. Seeger, R. Cochran, and O. Ghribi.** 2009. Broad DNA repair responses in neural injury are associated with activation of the IL-6 pathway in cholesterol-fed rabbits. J. Neurochem. **111:**1011–1021.
77. **Wu, M., W. L. Brown, and P. G. Stockley.** 1995. Cell-specific delivery of bacteriophage-encapsidated ricin A chain. Bioconjug. Chem. **6:**587–595.
78. **Wu, M., K. A. Harvey, N. Ruzmetov, Z. R. Welch, L. Sech, K. Jackson, W. Stillwell, G. P. Zaloga, and R. A. Siddiqui.** 2005. Omega-3 polyunsaturated fatty acids attenuate breast cancer growth through activation of a sphingomyelinase-mediated pathway. Int. J. Cancer **117:**340–348.
79. **Wu, M., Y. He, Y. Xu, M. Kobune, M. R. Kelley, and W. J. Martin II.** 2002. Protection of human lung cells against hyperoxia using the DNA base excision repair genes hOgg1 and Fpg. Am. J. Respir. Crit. Care Med. **166:**192–199.
80. **Wu, M., S. Hussain, H. Y. He, R. Pasula, P. A. Smith, and W. J. Martin II.** 2001. Genetically engineered macrophages expressing IFN-γ restore alveolar immune function in *scid* mice. Proc. Natl. Acad. Sci. U. S. A. **98:**14589–14594.
81. **Wu, M., M. R. Kelley, W. K. Hansen, and W. J. Martin II.** 2001. Reduction of BCNU toxicity to lung cells by high-level expression of O^6-methylguanine-DNA methyltransferase. Am. J. Physiol. Lung Cell. Mol. Physiol. **280:**L755–L761.
82. **Wu, M., R. Pasula, P. A. Smith, and W. J. Martin II.** 2003. Mapping alveolar binding sites *in vivo* using phage display peptide libraries. Gene Ther. **10:** 1429–1436.
83. **Wu, M., P. G. Stockley, and W. J. Martin II.** 2002. An improved Western blotting effectively reduces the background. Electrophoresis **23:**2373–2376.
84. **Yahr, T. L., J. Goranson, and D. W. Frank.** 1996. Exoenzyme S of Pseudomonas aeruginosa is secreted by a type III pathway. Mol. Microbiol. **22:**991–1003.
85. **Yoon, S. S., R. F. Hennigan, G. M. Hilliard, U. A. Ochsner, K. Parvatiyar, M. C. Kamani, H. L. Allen, T. R. DeKievit, P. R. Gardner, U. Schwab, J. J. Rowe, B. H. Iglewski, T. R. McDermott, R. P. Mason, D. J. Wozniak, R. E. Hancock, M. R. Parsek, T. L. Noah, R. C. Boucher, and D. J. Hassett.** 2002. Pseudomonas aeruginosa anaerobic respiration in biofilms: relationships to cystic fibrosis pathogenesis. Dev. Cell **3:**593–603.
86. **Zolfaghar, I., D. J. Evans, and S. M. Fleiszig.** 2003. Twitching motility contributes to the role of pili in corneal infection caused by *Pseudomonas aeruginosa*. Infect. Immun. **71:**5389–5393.

Editor: B. A. McCormick